Physica C 470 (2010) 1280–1283

Contents lists available at ScienceDirect

Physica C

journal homepage: www.elsevier.com/locate/physc

Spatially-resolved measurement on time-dependent electromagnetic behavior in alternating current carrying coated conductor

K. Higashikawa [a,*], Y. Honda [a], M. Inoue [a], M. Iwakuma [a], T. Kiss [a], K. Nakao [b], Y. Yamada [b], T. Izumi [b]

[a] Department of Electrical Engineering, Graduate School of Information Science and Electrical Engineering, Kyushu University, 744 Motooka, Nishi-ku, Fukuoka 819-0395, Japan
[b] Superconductivity Research Laboratory, International Superconductivity Technology Center, 1-10-13 Shinonome, Koto-ku, Tokyo 135-0062, Japan

ARTICLE INFO

Article history:
Available online 16 May 2010

Keywords:
Visualization
AC loss
Coated conductor
Magnetic microscopy

ABSTRACT

Establishment of processing technology for multifilamentary coated conductors (CCs) is a key issue for superconducting electric power applications from the viewpoint of AC loss reduction. On the other hand, CCs sometimes have local inhomogeneity in the superconducting layers, and that will cause a current blocking in a filament or inhomogeneity of critical current among filaments in a multifilamentary CC. Therefore, we need an assessment method for local electromagnetic behavior on AC loss properties of CCs. In this study, we developed a method for visualizing time-dependent AC loss distribution in CCs by using scanning Hall probe microscopy. We succeeded in visualizing local current density, electric field and loss density simultaneously with a spatial resolution of a few hundred micrometers. The measurement system has possible scanning area of 150×50 mm^2 and current capacity of 500 A. This enables us to discuss the local electromagnetic behavior on a practical scale of CCs. We believe that this visualization method will be a very powerful tool to estimate the feasibility of processing technology for multifilamentary CCs.

1. Introduction

Fabricating processes of $REBa_2Cu_3O_{7-\delta}$ (REBCO, RE: rare earth) coated conductors (CCs) such as $YBa_2Cu_3O_{7-\delta}$ (YBCO) and $GdBa_2Cu_3O_{7-\delta}$ (GdBCO) CCs have been developed steadily in recent years [1–4]. For example, SuperPower Inc. has achieved a 1065 m long CC with the minimum critical current of 282 A/cm [4]. Such a progress leads us to the next stage of the development of practical applications using CCs.

For electric power applications, on the other hand, forming multifilamentary configuration on CCs will also be a key technology from the point of view of AC loss reduction. For example, it has been reported that AC losses in CCs can be reduced by increasing the number of filaments [5–8]. This demonstrates the high applicability of CCs to electric power applications such as power transmission cables, transformers and superconducting magnetic energy storage.

However, it has also been reported that CCs sometimes have local defects and inhomogeneity in the superconducting layers [9,10]. In case of monofilamentary CCs, e.g., 10-mm-wide CCs, that does not largely influence the total performance because current can flow around such defects. In case of multifilamentary CCs, on the other hand, that will cause a significant current blocking in a filament or inhomogeneity of critical current among filaments. In such cases, we cannot discuss the electromagnetic behavior only from a general AC loss estimation such as the four-probe method and pick-up coil method because we can only detect global loss integrating whole period. Therefore, for the establishment of the processing technology for multifilamentary CCs, we need an assessment method to understand the local electromagnetic behaviors on AC loss properties of CCs.

In this study, we developed a visualization method of time-dependent AC loss distribution in CCs by using scanning Hall probe microscopy. We tried to visualize local current density, electric field and loss density in a multifilamentary model sample of a YBCO CC under alternating transport current.

2. Methods

2.1. Sample

Fig. 1 shows an optical micrograph of the sample. The sample was prepared from a 10-mm-wide YBCO CC, and was processed by photolithography and wet etching. Ten filaments were patterned on a 5-mm-wide and 8-mm-long area, and the width of each filament was 340 μm. Furthermore, some failures such as bridges, disconnections and defects were purposely simulated on

* Corresponding author. Address: Kiss Laboratory, Department of Electrical and Electronic Systems Engineering, Graduate School of Information Science and Electrical Engineering, Kyushu University, 744 Motooka, Nishi-Ku, Fukuoka 819-0395, Japan. Tel.: +81 92 802 3678; fax: +81 92 802 3677.
E-mail address: kohei@super.ees.kyushu-u.ac.jp (K. Higashikawa).

0921-4534/$ - see front matter © 2010 Published by Elsevier B.V.
doi:10.1016/j.physc.2010.05.093

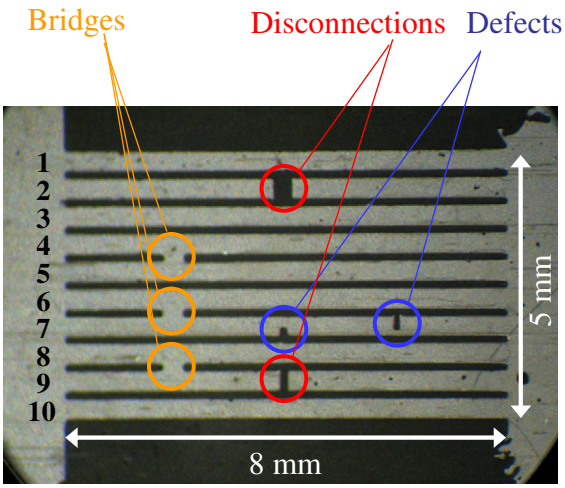

Fig. 1. Optical micrograph of the sample. Ten filaments were patterned on a YBCO coated conductor. The widths of the filament and the gap were 340 μm and 160 μm, respectively. Furthermore, some failures such as bridges, disconnections and defects were intentionally simulated on the sample.

the sample. We used this sample as an example for the visualization method.

2.2. Measurement

Fig. 2 shows a schematic diagram of the measurement system. The system of the scanning Hall probe microscopy has two liquid nitrogen tanks. One is for current leads, and this enables current capacity of 500 A. The other is for cooling stage. The sample is cooled by heat conduction from the stage, and then a typical temperature of the stage becomes around 82 K. The Hall probe is located above the sample. The active area of the Hall sensor is 50 μm × 50 μm, and perpendicular component of magnetic field, B_z, generated by the sample is measured by this sensor. The Hall probe can be controlled with a spatial resolution of 1 μm, 1 μm and 0.25 μm in x, y and z directions, respectively.

A sinusoidal transport current was applied to the sample from a bipolar current source controlled by a function generator. For noise reduction, also the Hall sensor was biased by another channel of the function generator, and then the signal from the sensor was acquired through a lock-in amplifier. At a measurement point, B_z was measured during one cycle of the alternating transport current by synchronizing the transport current. Then, the Hall probe was moved to the next measurement point. These procedures were repeated for a whole measurement area, and eventually we could obtain in-plane distributions of B_z as a function of time.

2.3. Data analysis

If we assume in-plane 2D current distribution in the sample, i.e., sheet current density in xy-plane, $\boldsymbol{J}$, the distribution of $\boldsymbol{J}$ can be derived analytically from that of measured B_z based on the inverse problem of Biot–Savart law. Roth et al. have already reported a method for that, and x and y components of $\boldsymbol{J}$, J_x and J_y, are expressed in Fourier space as follows [11]:

$$\tilde{J}_x(k_x,k_y) = -i\frac{2}{\mu_0}\frac{k_y}{k}e^{kz_{\text{lift-off}}}\tilde{B}_z(k_x,k_y) \tag{1}$$

$$\tilde{J}_y(k_x,k_y) = i\frac{2}{\mu_0}\frac{k_x}{k}e^{kz_{\text{lift-off}}}\tilde{B}_z(k_x,k_y) \tag{2}$$

where $\tilde{J}_x$, $\tilde{J}_y$ and $\tilde{B}_z$ are the Fourier transformations of J_x, J_y and B_z, respectively. The variables k_x and k_y are the components of the wave number $\boldsymbol{k}$, and k is the absolute value of $\boldsymbol{k}$ given by $\sqrt{k_x^2+k_y^2}$. The constant $z_{\text{lift-off}}$ is the distance from the current sheet to the measurement point of B_z. According to the increment of $z_{\text{lift-off}}$, spatial harmonics of $\tilde{B}_z$ are weakened especially at large k. Eqs. (1) and (2) indicate that such harmonics should be amplified by the term of $e^{kz_{\text{lift-off}}}$ to restore the magnetic field just at the current sheet. However, at very large k, the harmonics are weakened down to a noise level of the measurement. This means that we should give up the information of such large k. Therefore, some low-pass filter should be used, and the Hanning window was used in this study. The cut-off wavelength, $\lambda_{\text{cut-off}}$, determines the spatial resolution of the distribution of $\boldsymbol{J}$.

Furthermore, the distribution of electric field, $\boldsymbol{E}$, can also be estimated from that of time-derivative B_z based on Faraday's Law. Dinner et al. have reported a method for that [12], and x and y components of $\boldsymbol{E}$, E_x and E_y, are expressed in Fourier space as follows:

$$\tilde{E}_x(k_x,k_y) = i\frac{k_y}{k^2}e^{kz_{\text{lift-off}}}\frac{\partial\tilde{B}_z(k_x,k_y)}{\partial t} \tag{3}$$

$$\tilde{E}_y(k_x,k_y) = -i\frac{k_x}{k^2}e^{kz_{\text{lift-off}}}\frac{\partial\tilde{B}_z(k_x,k_y)}{\partial t} \tag{4}$$

where $\tilde{E}_x$ and $\tilde{E}_y$ are the Fourier transformations of E_x and E_y, respectively. However, Eqs. (3) and (4) are valid only when the curl-free electrostatic portion, $\boldsymbol{E}_p$, is negligible compared with the divergence-free inductive $\boldsymbol{E}_i$ [12]. In this study, the transport current applied to the sample was 88% of the critical current of the sample at the maximum. In case of a typical CC, the corresponding electric field in steady state, i.e., the magnitude of $\boldsymbol{E}_p$, becomes two orders smaller than the electric field criterion. On the other hand, as a result of the measurement, the magnitude of $\boldsymbol{E}_i$ became the same order as the electric field criterion. Therefore, we did not consider $\boldsymbol{E}_p$, and used Eqs. (3) and (4) for the estimation of the distribution of $\boldsymbol{E}$.

In this way, we can estimate the distributions of $\boldsymbol{J}$ and $\boldsymbol{E}$ from the measurement of B_z. That means that we can finally obtain loss density, q, by considering the inner product of $\boldsymbol{J}$ and $\boldsymbol{E}$:

$$q = J_xE_x + J_yE_y. \tag{5}$$

3. Results and discussion

Fig. 3 shows the distributions of measured magnetic field, sheet current density, electric field and loss density as a function of time. An alternating transport current, I, with an amplitude of 30 A was applied to the sample in x direction with a frequency of 2 Hz. The critical current, I_c, of the sample defined with the electric field criterion of 0.1 mV/m (1 μV/cm) was 34 A at this temperature. Therefore, the maximum load factor (I/I_c) was 88% for these results. The time, t, is defined as zero at the zero phase of the transport current, and then the time cycle becomes 500 ms. Furthermore, these images were obtained with $\lambda_{\text{cut-off}}$ = 230 μm.

A positive current flowing in x direction should generate a positive value of B_z in the upper region and a negative value of B_z in the lower region. Such distributions of B_z were obtained at t > 70 ms. However, the situation was opposite at t < 30 ms in the middle part of the sample while the total transport current was positive in x direction. For this sample, all filaments were coupled because they were connected with each other at both ends of the sample. Therefore, it can be understood that such opposite distributions are formed as a result of magnetic flux trapped from a negative transport current in the previous cycle of the alternating transport current. This kind of trap can also be confirmed from the fact that B_z keep similar distribution in the middle part of the sample at t > 120 ms while the transport current largely decreases from the peak value.